Nuclear Engineering and Design 324 (2017) 78–92

Contents lists available at ScienceDirect

Nuclear Engineering and Design

journal homepage: www.elsevier.com/locate/nucengdes

CFD analysis of the impact of a novel spacer grid with longitudinal vortex generators on the sub-channel flow and heat transfer of a rod bundle

J.M. Wu*, H.Y. Liang, F.J. Zhu, J. Lei

State Key Laboratory for Strength and Vibration of Mechanical Structures, Shaanxi Key Laboratory of Environment and Control for Flight Vehicle, School of Aerospace, Xi'an Jiaotong University, Xi'an City, Shanxi Province 710049, China

ARTICLE INFO

Keywords:
Longitudinal vortex generator
Spacer grid
Fuel assembly
Thermal-hydraulic characteristics

ABSTRACT

In this study, a novel spacer grid with rectangular wing longitudinal vortex generators (RLVGs) is designed to improve the thermal–hydraulic characteristics of fuel assembly and simplify the spacer grid structures. The impacts of the attack angle (30°, 45°and 60°) and the distribution (two patterns) of RLVGs on the thermal–hydraulic characteristics in the sub-channels of a rod bundle are numerically investigated. Numerical results show that the secondary flow generated by the RLVGs can spread to the downstream region of spacer grid, disturb the boundary layer of the rods and improve the heat transfer of coolant. For the novel design of pattern 1, the spacer grid with RLVGs in attack angle of 45° generates secondary flow around the fuel rods just like a circulating flow in higher velocity, resulting better heat transfer performance and uniform cooling of fuel rods. Based on these results, a novel design of pattern 2 with doubled RLVGs number of pattern 1 is introduced and numerically investigated too. With the same attack angle of 45°, pattern 2 increases the average transverse velocity of the secondary flow and decreases the rod wall temperature in comparison with those of pattern 1 at the same Reynolds number conditions. Maximum increase in Nusselt number in the sub-channels is up to 30% while the increase in the total pressure drop is about 7.6% comparing with those of pattern 1. The present results indicate that the novel design of pattern 2 is an efficient way on improving the heat transfer of the fuel rod bundle, deserving more work to optimize its geometry structure and distribution before practical application.

1. Introduction

The safety and economy characteristics of a nuclear power plant are greatly influenced by the thermal-hydraulic characteristics of fuel assemblies. As one of the essential components in fuel assemblies, the spacer grid is designed to support the fuel rods mechanically, reduce the flow-induced vibration, as well as generate secondary-flow in sub-channels and improve the thermal-hydraulic performance of the rods fuel assembly.

Spacer grid with different mixing vanes is often used in fuel rod assemblies to create a specific coolant mixing behavior by increasing the turbulence level and guiding the transverse flow to further downstream of the grid in the fuel rod sub-channels. Specifically designed vanes on the spacer grid have great effects on the turbulence level and the secondary flow pattern in the sub-channels of fuel rod bundle. Fig. 1 shows a typical spacer grid used in the fuel rod assembly of pressurized water reactors (PWR) (Su et al., 2013). So far, considerable work has focused on the performance of fuel assemblies with mixing grids. Holloway et al. (2008) experimentally investigated the performance of the convective heat transfer in rod bundles with three different type of spacer grids (split-vane pair support grids, disc support grids, and standard support grids). It was found that the local heat transfer was enhanced by the support grids. For the support grids with split-vane pair, heat transfer enhancement was also found further downstream of the spacer grid at a distance of as much as 10 times the hydraulic diameter of sub-channel. To understand the turbulent flow characteristics in the sub-channel of fuel rod bundle with split type and swirl type mixing vanes, respectively, Chang et al. (2008) observed the velocity distribution in the sub-channel using a two-component Laser Doppler Anemometry (LDA). The results showed that the mixing vanes (split type and swirl type) increased the turbulent intensities of the flow at the center of sub-channels. The turbulent intensities decayed quickly in the downstream of spacer grid for both types of mixing vane. The flow mixing between the neighboring sub-channels was stronger than the mixing within a sub-channel for the case with a split type spacer grid. While for the case with swirl type spacer grid, the opposite had occurred. At just behind the spacer grid, split type vanes generated stronger turbulent intensity than swirl type vanes did. Han et al. (2009)

* Corresponding author.
E-mail address: wjmxjtu@mail.xjtu.edu.cn (J.M. Wu).

http://dx.doi.org/10.1016/j.nucengdes.2017.08.029
Received 20 March 2017; Received in revised form 10 July 2017; Accepted 26 August 2017

Nomenclature

C_d	Resistance factor
D_e	Hydraulic diameter of sub-channel, m
Nu	Nusselt number
p	Static pressure, Pa
v	Transverse velocity, ms^{-1}
T	Bulk temperature of coolant, K
T_w	Wall temperature of rods, K

Greek symbols

α	Attack angle of RLVG, °

Abbreviations

LVG	Longitudinal vortex generator
RLVG	Rectangular wing longitudinal vortex generator

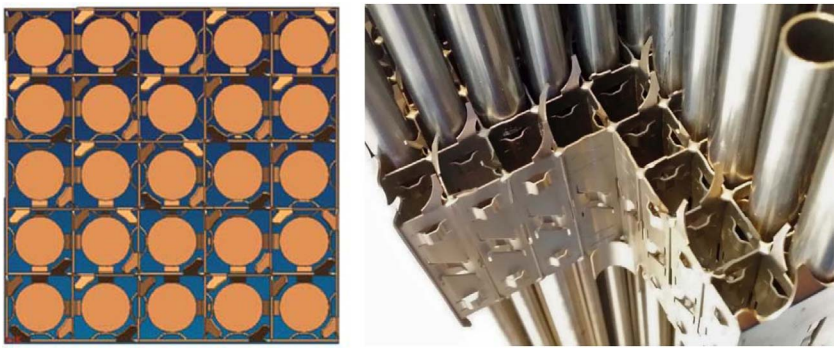

Fig. 1. Typical structures of the spacer grid used in the rods fuel assembly.

designed a new type of vane (Tandem Arrangement Vane, TAV) and experimentally studied the flow features in the cross sections of a 6 × 6 rod bundle with that design. The results showed that the swirling flow generated by the designed vane could be maintained in the downstream of spacer grid up to 20 times the hydraulic diameter of sub-channel.

As we know, the geometric structure of the spacer grid with different mixing vanes is relatively complicated, twisted and with many narrow gaps. The detailed flow characteristics in these narrow gaps is hard to be detected by experiment. However, Computational Fluid Dynamics (CFD) method is greatly helpful to get the flow details in this kind of complex structure. The effect of the spacer grid with different mixing vanes on the sub-channel flow and heat transfer of a fuel rod bundle is being increasingly investigated with the rapid development of CFD technologies. Nematollahi and Nazifi (2008) carried out a CFD analysis to examine the flow characteristics in the sub-channels, the overall heat transfers and pressure drops of a fuel assembly with different mixing vanes on the spacer grid. In the simulation, a standard k-ε model was used. An increase of 9.82% in the total heat transfer of the case with split vanes on the spacer grid was found and deemed reasonable, however, the pumping cost increases with considering the manufacturing possibility. The critical heat flux (CHF) phenomenon in a 2 × 3 rod bundle with different mixing vanes (split, swirl and hybrid types) was tested at KAIST R-134a Loop and numerically analyzed by CFX in Shin and Chang's work (Shin and Chang, 2009). It was found that mixing vanes could bring about an increase in CHF, especially under the conditions with higher mass flux and lower pressure. This is because the secondary flow generated by the mixing vane on the spacer grid flattened the void fraction distribution and decreased the maximum value of void fraction. Under the conditions with lower pressure and smaller mass flux, the swirl vane had the highest performance. Under PWR operating conditions, the hybrid vane had the best performance. Tóth and Aszódi (2010) investigated the flow field numerically in the sub-channels of fuel assemblies used in VVER-440, a pressurized water reactor designed by Russian, to examine the applicability of turbulence models (k-ε, SST k-ω, BSL and SSG Reynolds stress models) in modeling the sub-channels. A triangular configuration was adopted to arrange the fuel rods in VVER-440. It should be noted that no spacer grid was enclosed in the selected geometrical model. Obviously this is not the situation of the rod bundle's sub-channels in practical reactors. It was concluded that the BSL model could capture the turbulence flow characteristics rather well in the sub-channels by comparing the numerical results with experimental data. Conner et al. (2010) developed a CFD methodology using the STAR-CD code to predict the flow characteristics and heat transfer in PWR fuel assemblies behind the spacer grids with mixing vanes. The computational domain included one span length of a 5 × 5 fuel rod bundle, spacer grid with springs and mixing vanes. The renormalization group (RNG) k-ω model was used with y^+ value of 40–100. The numerical results and the methodology were validated by small-scale experiment data obtained under low Reynolds number and low temperature conditions. Gandhir and Hassan (2011) numerically investigated the effect of the structural spacer grid with concept mixing vanes on the flow characteristics of the downstream of the spacer grid in a 5 × 5 fuel rod bundle. In this steady and isothermal simulation, turbulence models of realizable k-ε and SST k-ω, and an open source code were used. The results showed that SST k-ω predicted pressure drop more accurate than realizable k-ε did. Liu et al. (2012) utilized CFD to examine the turbulence models and wall treatment, mesh refinement and boundary conditions in modeling the fluid dynamics and heat transfer in sub-channels of a rod bundle with split vanes on the supporting grid. It was suggested that the near-wall treatment method and mesh were of great importance in determining the turbulent models best suited to simulate the flow feature in rod bundle sub-channels. In their flow conditions, the SST k-ω turbulence model with standard wall function could predict the Nusselt number near the walls with higher accuracy. However, the realizable k-ε turbulence model was considered to be able to predict the surface heat transfer very well by integrating the enhanced wall treatment method. Jayanti and Rajesh (2013) numerically investigated the characteristics of vapor single phase flow and heat transfer through the rods bundle channels (with spacer grid but without mixing vane) by CFX code. Eulerian–Lagrangian approach was used to solve the gas-droplet two-phase flow. The droplets deposition and film formation on the spacer

grid were calculated. The film formed on the grid were thought to be torn into ligaments and broken to smaller droplets by the vapor flow with high speed. The smaller droplets might deposit onto the rods or re-enter the vapor main flow. Smaller droplets could evaporate more quickly than larger ones, increasing the evaporating heat transfer and decreasing the rods wall temperature. This is a potential explanation to why spacer grids enhance the heat transfer coefficient and CHF of fuel assemblies. Zhu et al. (2014) numerically studied the supercritical water flow features in a triangular tight rod bundle with a standard spacer grid or a spacer grid with split vanes. After numerous tests on the applicability of turbulence models, the standard two layer k-ε model was applied to simulate the supercritical water flow in the rod buddle sub-channels, in which the value of y^+ is less than 1. The results showed that the heat transfer was decreased at the downstream of spacer grid in this tight rod bundle's sub-channels for both standard and split-vane cases. It was concluded that the local heat transfer enhancement region just behind the grid should be enlarged by increasing the local velocity around the spacer grid in designing the fuel assemblies. In Tseng et al. (2014)'s simulation work, the thickness of spacer grid and vane-pair was considered in their geometry model. The total heat generation rate inside the rods was assigned to handle the fuel rods' surface boundary condition, rather than constant heat flux as in other open literature. Turbulence model of SST k-ω was applied to examine the flow and heat transfer behaviors in the sub-channels of fuel rod bundle. The circumferential variation in Nu number around the rods was explained as flow impingement on (higher) or detachment from (lower) the rods' surface, which was induced by the split-vane pair's swirling effects. Bieder et al. (2014) used LES based on Trio_U code to investigate the flow characteristics in the sub-channels of fuel assemblies. Their computational domain consisted of two successive spacer grids with mixing vanes, while in the majority of previous simulation work, only one spacer grid was included. The results showed that the effect of cross flow velocity induced by the first grid would continue to the second grid. In the proximity less than 10 times of sub-channel's hydraulic diameter away from the grid, the mean velocities of the sub-channels predicted by LES or k-ε models matched the experimental data very well. However, in the far downstream of grid, isotropic turbulent feature occurs, linear turbulent viscosity models such as k-ε models were no longer suitable. This nonlinear eddy viscosity might be accounted for by LES, but nonphysical results could be caused as well. As a blind benchmark exercise based on the KAERI experimental data, Podila et al. (2014) detailed their simulation work about the water flow features in a rod bundle with a split-type spacer grid. Taking into account of the flow interaction between the neighboring sub-channels, a whole 5 × 5 rod bundle were included in their computational geometry model to capture the turbulence characteristics comprehensively. In order to achieve convergence easily, standard k-ε model was employed first and then the Reynolds stress model (RSM) was utilized to predict the anisotropic behavior of turbulent behind the grid. It was found that the turbulence intensity values were under predicted, while the trends of the three velocity components were predicted rather well compared to the experiments. A finer mesh in the spacer grid and along the axial flow direction was suggested to predict the flow details. Also as a blind benchmark exercise, a segregated turbulence model has been applied in Chang and Tavoularis's (2015) work to model the turbulent feature in the sub-channels of fuel assemblies with split-vanes. The cross section of their computational domain consists of three sub-channels: an inner, an intermediate and a wall sub-channel. The axial length of their computational domain was 27.1 times of sub-channel's hydraulic diameter which were divided into three sections: upstream bare rod bundle section, spacer grid section and downstream bare rod bundle section. In the upstream and downstream domains, Scale Adaptive Simulation (SAS) turbulence model was used, while LES model was used in the spacer grid domain to reduce the mesh number in the entire domain. The vortex structures generated by vanes are detected and analyzed inthe flow near the vanes. The evolution of the induced vertices in the downstream of the spacer grid was identified and explained. Krapivtsev et al. (2015) numerically investigated the flow heat transfer characteristics in the rod bundle with modified cell-type spacer grids to be used to Russian reactors. The modified cell-type spacer grids were designed as cells with three elastic corrugated wall in the same inclinations (type 1) or three elastic corrugated wall with different inclinations and arranged in alternating rows (type 2), to generate the secondary flows around the fuel rods or between the rows. The results showed that the secondary flows generated by type 1 spacer grid were counter-clockwise around the rods. While the secondary flows generated by type 2 spacer grid were in the same direction in the gaps between the neighboring rods, but in different direction in different gaps. Both two types of spacer grids could even the temperature distribution across the rod bundle by the generated secondary flows. The subcooled boiling phenomenon in the rod bundle channels were simulated in Zhang et al's. (2015) work by employing Eulerian two-fluid and wall boiling models. The results indicated that vapor volume fractions and temperature on the rod wall were greatly decreased by the mixing effect of vanes, and CHF increases. Capone et al. (2016) provided a modeling method to handle the morphology complexity of spacer grids with dimples, springs and mixing vanes as momentum source terms in simulating the flow in the entire domain of a rod bundle to reduce the meshing difficulties and computing cost. Obviously, how to obtain the momentum source terms to feature the presence of dimples, springs and vanes is one of key steps for the accuracy of this method. Capone et al. detailed their implementation on this topic. The authors stated that the method should be validated by experimental data. As a continuing work of Podila et al. (2014), Podila and Rao (2016) presented their results to assess the impacts of upstream length of the grid, mesh fineness in the grid zone and applicability of turbulence models in predicting the turbulence features in the rod bundle with split-type vanes. An interesting finding was that turbulence models had no effect on the calculated turbulence intensities. Turbulence intensities were underestimated compared with experimental data. Agbodemegbe et al. (2016) adopted Realizable k-ε model, standard k-ε model and SST k-ε model to investigate the flow in the rod sub-channels with mixing vanes. The results showed that Standard k-ε model and the SST k-ε model can better capture the change of turbulent flow field. The numerical results had a good agreement with the experimental data.

In brief, the turbulence flow in the rod bundle with spacer grid is a continuing research interest in the field of the thermal-hydraulics in nuclear cores. The objectives are to capture the turbulence features and improve the mixing and uniformity of flow and heat transfer downstream of spacer grid. Similar to the mixing vanes on the spacer girds in the fuel rod bundle, the vortex generator (VG) on solid surfaces also can induce swirls and destabilize the flow. Vortex generators (VGs) were first introduced to control boundary layer and reduce the flow loss (Schubauer and Spangenberg, 1960). Johnson and Joubert's (1969) first presented the effects of VG on heat transfer characteristics. Longitudinal vortex generator (LVG) can generate the secondary flow with rotating axes parallel to the main stream, named longitudinal vortex (LV). LVs spiral and persist long distance along the stream. A large number of research is focused on the heat transfer enhancement of air compact heat exchanger by punching out or mounting LVGs on the fin surface since the 1990 s. The type, size, position and orientation of LVGs on the plain fin or other enhanced fin surfaces (wavy fin, dimple fin, etc.) with different tube types (round, flat and oval) in Ahmed et al. (2012) have been reviewed. In our previous work, the inherent mechanism of heat transfer by the LVGs was firstly interpreted from the viewpoint of field synergy principle (Wu and Tao, 2007). The

intersection angle between the velocity and temperature gradient is decreased, while velocity and temperature fields become more synergistic for convective heat transfer by the secondary flow generated by LVGs. In previous practices, heat transfer enhancement accompanied by less increase in pressure drop could also be expected by appropriate design of LVGs.

The objective of this study is to numerically investigate the flow and heat transfer characteristics in the sub-channels of a fuel rod bundle with a novel designed spacer grid. The novel spacer grid uses rectangular wing longitudinal vortex generators (RLVGs) instead of the traditional mixing vanes to generate the secondary flow in the sub-channels. The impacts of the attack angle (30°, 45 °and 60°) and the distribution (two patterns) of RLVGs on the thermal-hydraulic characteristics of the sub-channels flow and heat transfer are checked.

2. Numerical methodology

2.1. Geometry model and calculation domain

Fig. 2 shows the structure and sizes of a 5 × 5 spacer grid with RLVGs, which is made of Zircaloy-4 and designed on the basis of traditional spacer gird. In which, simple RLVGs are just punched out from the straps of grid vertically, instead of mixing vanes in the traditional spacer gird. The attack angle of RLVGs is denoted by α. Fig. 2(a) shows a geometrically periodic length of a fuel rod bundle. Fig. 2 (b) gives a 3D zoom view of the novel spacer grid. A pair of RLVGs with different orientation are punched out from the opposite grid's straps for every grid cell. This design is named pattern 1 hereafter. The arrangement of RLVGs in the neighboring grid cells is staggered, so as to generate the longitudinal vortices with the same rotation direction when coolant flows cross the RLVGs in the rod sub-channel formed by 4 quarter rods. Fig. 2(c) and (d) show the sizes of the spacer grid and RLVG. The geometry sizes of the RLVGs is limited by the geometry structure sizes of the rod bundle.

Considering the distribution features of RLVGs and the large length size of the rods, a simplified calculation domain shown as Fig. 3 is used to avoid an unbearable mesh number. Actually, the calculation domain consists of four sub-channels, formed by 4 half rods, 4 quarter rods and 1 full rod, spacer grid and RLVGs. In the main flow direction (Y direction), a geometrically periodic length shown in Fig. 2(a) is included in the selected calculation domain. In this domain the upstream length of the spacer grid is 5 mm, and the total length of the fuel rod bundle is 520 mm. The impacts of LVGs on the heat transfer and flow characteristics in the sub-channels of rod bundle are investigated.

2.2. Models and boundary conditions

The flow is taken as steady, incompressible one. The governing equations include mass, momentum and energy equations for coolant region, and conduction equation for solid spacer grid region. They are omitted here. For the first step the simulation of the case of pattern 1 design used standard k-epsilon model with enhanced wall function method to get rapid convergent numerical results. Based on these results, an improved design of pattern 2 was proposed. Turbulence models of standard k-epsilon, SST k-ω and Reynolds stress model (RSM) are used for the simulations of pattern 2 design. The numerical results are compared to check the sensitivity of turbulence models on the CFD predictions of this kind of sub-channel flow.

In this study, we just want to understand the impact of RLVGs on the flow and heat transfer in the sub-channels of a rod bundle. The adopted boundary conditions are simplified. That is, the inlet is set to be velocity inlet boundary, the outlet is set to be pressure outlet boundary. Constant heat flux of 0.5 MW/m^2 and no-slip conditions are assigned to the entire walls of the fuel rods. As shown in Fig. 3, the left and right side boundaries of the coolant sub-channels are set to be geometric periodicity boundary condition 1, while the top and the bottom side

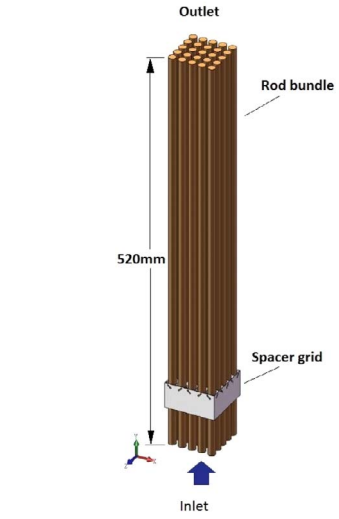

(a) Partial rod bundle

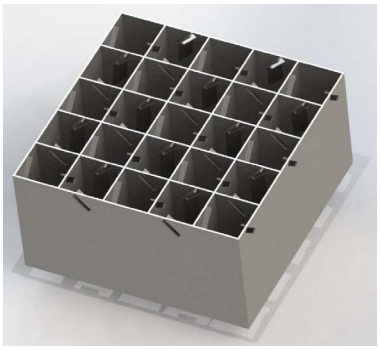

(b) 3D zoomed view of the spacer grid with punched RLVGs-pattern 1

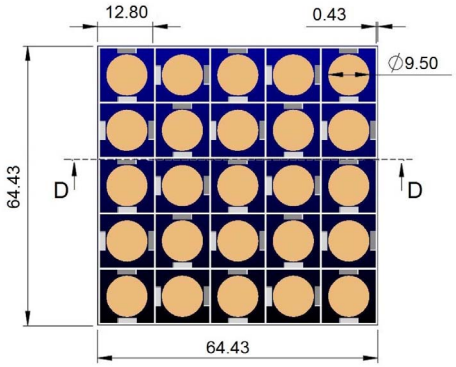

(c) Top view (Unit: mm)

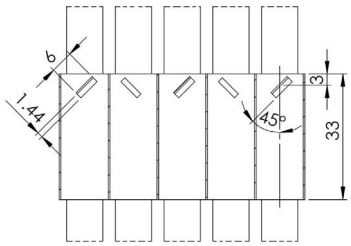

(d) D-D section view (Unit: mm)

Fig. 2. The schematic of the spacer grid with RLVGs.

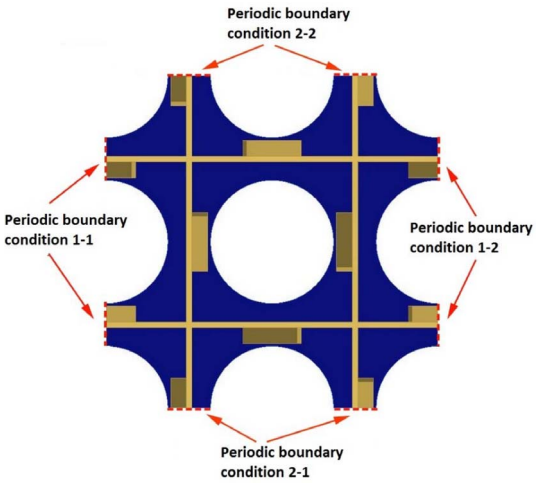

Fig. 3. The schematic of the simplified computation domain.

Table 1
Boundary conditions.

Boundaries	Boundary type	Values
Inlet	Uniform velocity/temperature	3,5,6,7,8 m/s 313.15 K
Outlet	Pressure outlet	1 atm
Wall surfaces of rods	Wall with uniform heat flux	0.5 MW/m^2
Left and right side boundaries	Periodic	
Top and bottom side boundaries	Periodic	

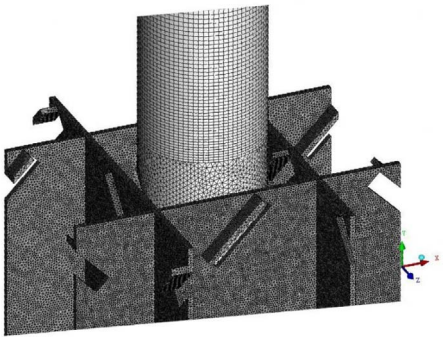

(a) Hybrid mesh in the region with spacer grid and the downstream with bare rod

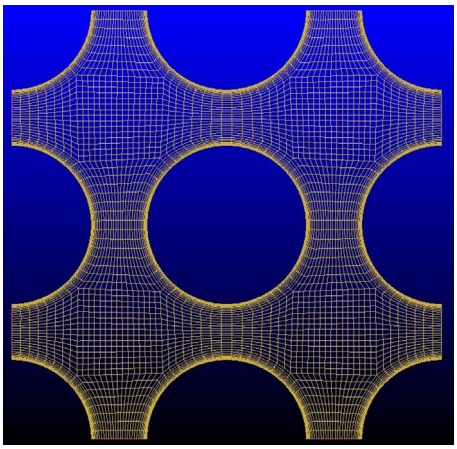

(b) Mesh in the cross section of sub-channels with boundary layers around the rods

Fig. 4. Generated mesh.

boundaries of the coolant sub-channels are set to be geometric periodicity boundary condition 2. Detailed boundary conditions are listed in Table 1.

ANSYS FLUENT 17.0 code was used for the CFD analysis in the present study. In order to take the heat conduction through the straps of the spacer grid into consideration, the thickness of the straps and the thermal conductivity of the material, Zircaloy-4 alloy, are considered. In ANSYS, the spacer grid with punched RLVGs is defined as solid with its own thermal conductivity, a very large value of viscosity is automatically assigned to the solid region. The thermal coupled wall surfaces are adopted for the coincident wall of the solid region and the fluid region. The thermal conductive equation in the solid region and the mass/momentum/energy equations in the coolant region are coupling solved. The convection terms are discretized using the second order upwind scheme, while the diffusion terms are discretized using the central difference scheme. SIMPLEC algorithm is chosen to solve pressure-velocity coupling equations. The residual value of the continuous equation is set to be 10^{-4}, the residual values of the momentum equation, k and ε equations are all set to be 10^{-6}, and the residual value

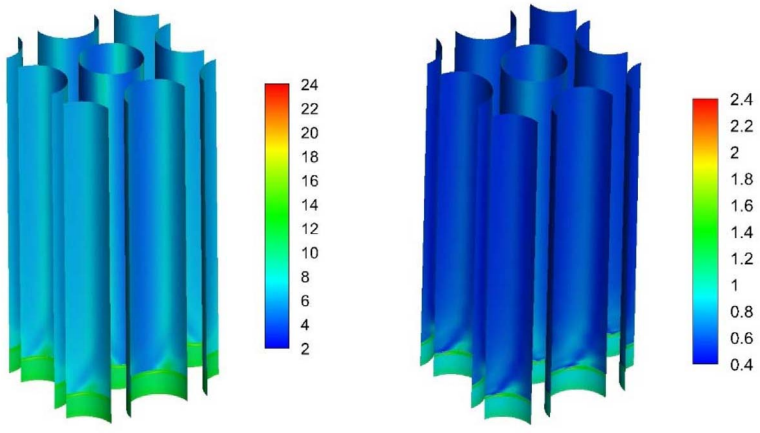

(a) For k-ε model (b) For SST k-ω and RSM models

Fig. 5. y+ distribution for different turbulence models.

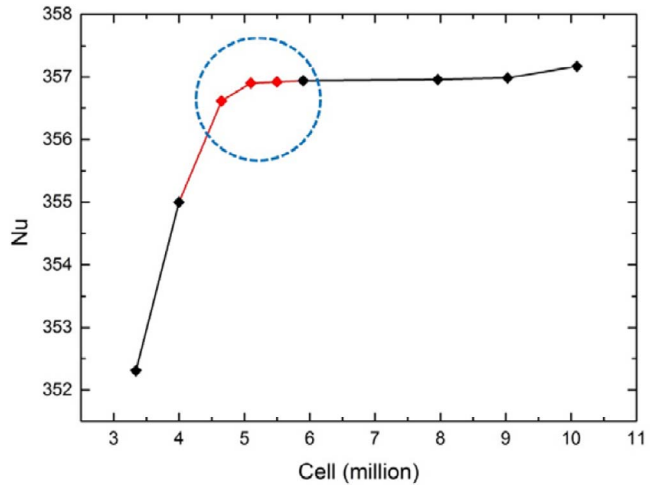

Fig. 6. Grid independence analysis.

of the energy equation is set to be 10^{-8} for the convergent solutions.

2.3. Mesh and check

ICEM CFD code was used to generate hybrid mesh in this study. It is hard to generate the boundary layers in the spacer grid mesh because of its complicated structure. Only on the rod wall surfaces there are boundary layers. However, the generated tetrahedral mesh near the spacer grid has exactly the same size with the first layer mesh on the rod wall surface, shown in the Fig. 4, to make sure the mesh fine enough. A pair of "interfaces" are used to exchange data in the junctions of two sets of mesh. Along the thickness direction of spacer grid with punched RLVGs, 3 layers of mesh are generated. The suitable y+ value is dependent on the turbulent model adopted. In the mesh work, this should be noted. The k-ε model with enhanced wall function method used in our primary simulation requires the values of y+ range from 1 to 30. Fig. 5(a) shows the y+ distribution of the generated mesh for the calculation using the k-ε model with enhanced wall function method. One can find that the y+ values are about 6–14. For SST k-ω and RSM models, the suitable y+ value is about 1. Fig. 5(b) shows the y+ distribution of the generated mesh for the calculation with using SST k-ω and RSM models. One can find that the y+ values are about 1. Thus, the values of y+ meet the requirement of different turbulent models adopted in present study.

To obtain the mesh independent results, nine sets grid systems with mesh number from 3.34 million to 10.09 million are applied and checked. Fig. 6 compared the average Nusselt numbers of the whole flow field for the different grid systems. The numerical results show that the average Nusselt number is almost unchanged after the mesh number exceeds 5.12 million. Thus the grid system with grid cells of 5.12 million is used in the following simulation.

2.4. Data post-processing

To gain the Nusselt number variation along Y direction, the computation domain is cut with many transverse planes and marked with different Y values. For every single small section between the two neighboring cross sections, the Nusselt number computed according to the following equations could be taken as the local Nusselt number in the middle location of this section.

$$Nu = \frac{hD}{\lambda} \tag{1}$$

$$h = \frac{q}{T_b - T_w} \tag{2}$$

In which, h is the convective heat transfer coefficient between the rod walls and coolant, D is the hydraulic diameter of the sub-channel, while λ is the thermal conductivity of the coolant, q is the heat flux, T_b is the bulk temperature of the coolant in this section, while T_w is the area averaged temperature of the rod wall in this section.

2.5. Sensitivity analyses of the influence of upstream length of spacer grid on the flow predictions

The objective of this study is to investigate the effect of the novel spacer grid on its downstream flow and heat transfer in the sub-channels of a fuel rod bundle. Thus short upstream length of 5 mm in our

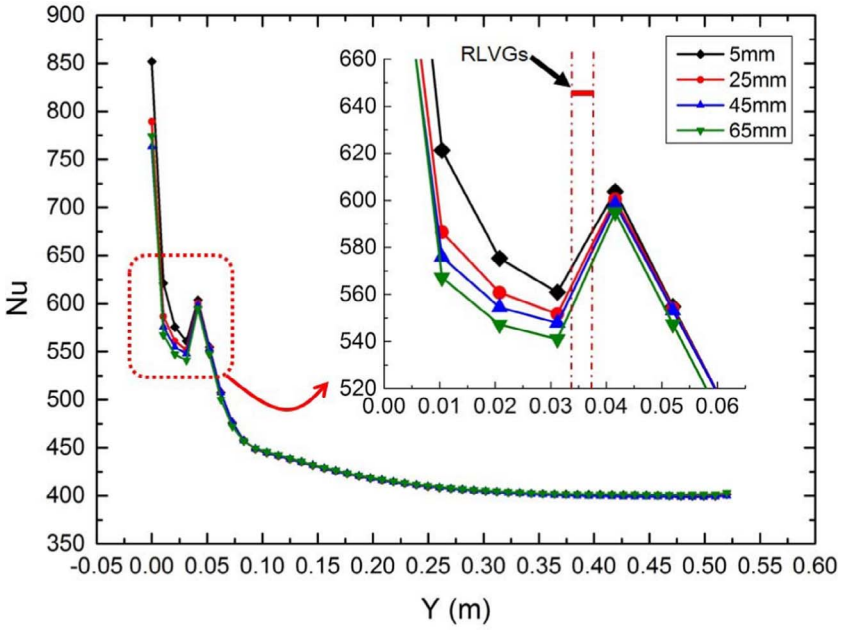

Fig. 7. The effect of the upstream length of spacer grid on the Nu along Y direction.

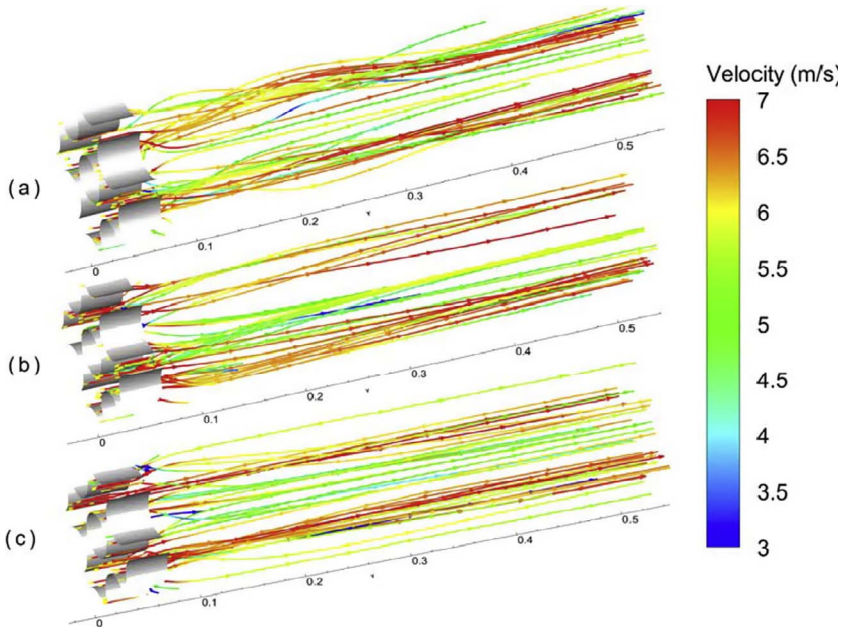

Fig. 8. Streamlines cross the RLVGs with different attack angles (a) $\alpha = 30^{\circ}$, (b) $\alpha = 45^{\circ}$, (c) $\alpha = 60^{\circ}$.

original computational domain was selected to reduce the amount of calculation work. To check the sensitivity of the upstream length of spacer grid on the predicted results, another three cases with enlarged upstream length (25, 45 and 65 mm) of spacer grid are also numerically simulated. Thus the total lengths of the computational domain for these three cases are 540, 560 and 580 mm. It should be noted that the rod wall surfaces in the enlarged sections for these three cases (means the first 20 mm length of rods surface from the flow entrance for the 1st enlarged case, the first 40 mm length of rods surface from the flow entrance for the 2nd enlarged case, the first 60 mm length of rods surface from the flow entrance the 3rd case) are assigned isothermal condition. The other rod wall surfaces keep the constant heat flux condition. Also the other boundary conditions are kept the same as those of the original case. The predicted local Nusselt number along the axial direction for the three cases with enlarged upstream length are compared with that of the original case in Fig. 7. For the convenience of comparison, identical Y coordinate values for the spacer grid as the original case are taken for the three cases, therefore the enlarged upstream lengths for the three cases have negative Y values. It is found that the upstream length of the spacer grid only affects the local heat transfer of spacer grid. With the increase of the upstream length, the local heat transfer is decreased. This is due to that the spacer grid is located in the entrance section of the sub-channels with the influence of the developing velocity. While the upstream length of the spacer grid has less effect on the heat transfer of the sub-channels in downstream of the spacer grid. That is because that the strong secondary flow generated by RLVGs after the spacer grid dominates the flow and heat transfer characteristics. Thus, in the following simulation, the upstream length of spacer grid is kept 5 mm to reduce the amount of calculation work.

3. Results and discussion

3.1. Results and analysis for the design of pattern 1

As a first try, we carried out the numerical computation to obtain the flow and heat transfer characteristics in the rod sub-channels with RLVGs spacer grid of pattern 1 as shown in Fig. 3. The streamlines of coolant in sub-channels at different attack angles of RLVGs is shown in Fig. 8 on condition of Re = 93600 (The inlet velocity is 6 m/s.). It can be seen from Fig. 8 that the streamlines are neatly ordered and paralleled with each other at the upstream of RLVGs. After the RLVGs of the spacer grid, the direction and magnitude of the coolant velocity change along streamwise direction. The coolant flows in a manner of helical line. That means longitudinal vortices are generated when coolant flows across the RLVGs.

Along the streamwise direction, the coolant inlet is at Y = 0. The RLVGs are located at Y = 32 mm. The secondary flow at different cross section of Y = 80 mm, 160 mm, 240 mm, and 320 mm is checked to know the intensities of the generated longitudinal vortices. Fig. 9 shows the transverse velocity vectors at these cross sections for the case with RLVGs attack angle of 60° and Reynolds number of 93600 (The inlet velocity is 6 m/s.). One can find from Fig. 9 that two distinguished vortices in the sub-channels located in the lower left and upper right corners, respectively, are observed behind the RLVGs. While in the sub-channels located in the upper left and lower right corners, the secondary flow is not strong. Non-uniform cooling to the fuel rods may be resulted in because of this. The intensity of transverse flow is weakening gradually along the Y direction. The velocity near the fuel rod walls is larger. This may thin the thickness of boundary layer, enhance the cooling efficiency to the rod bundle and decrease the local rod wall temperature. Fig. 10 shows the generated vortices for the case with RLVGs attack angle of 45°. It is interesting to find that secondary flow around the fuel rods just like a circulating flow in higher velocity. The transverse velocity in the sub-channels located in the lower left and upper right corners is smaller in comparison with that of 60°, but more uniform in the four sub-channels. This could generate uniform cooling of fuel rods.

Figs. 11-13 gives the other results for the case with RLVGs attack angle of 45° and inlet velocity of 6 m/s. The maximum transverse velocity on different cross sections along the Y direction is shown in Fig. 11. It is found that the local transverse velocity of coolant just behind the RLVGs has a maximum value as high as about 2.2 m/s due to the generated vortices. The transverse velocity declines rapidly then

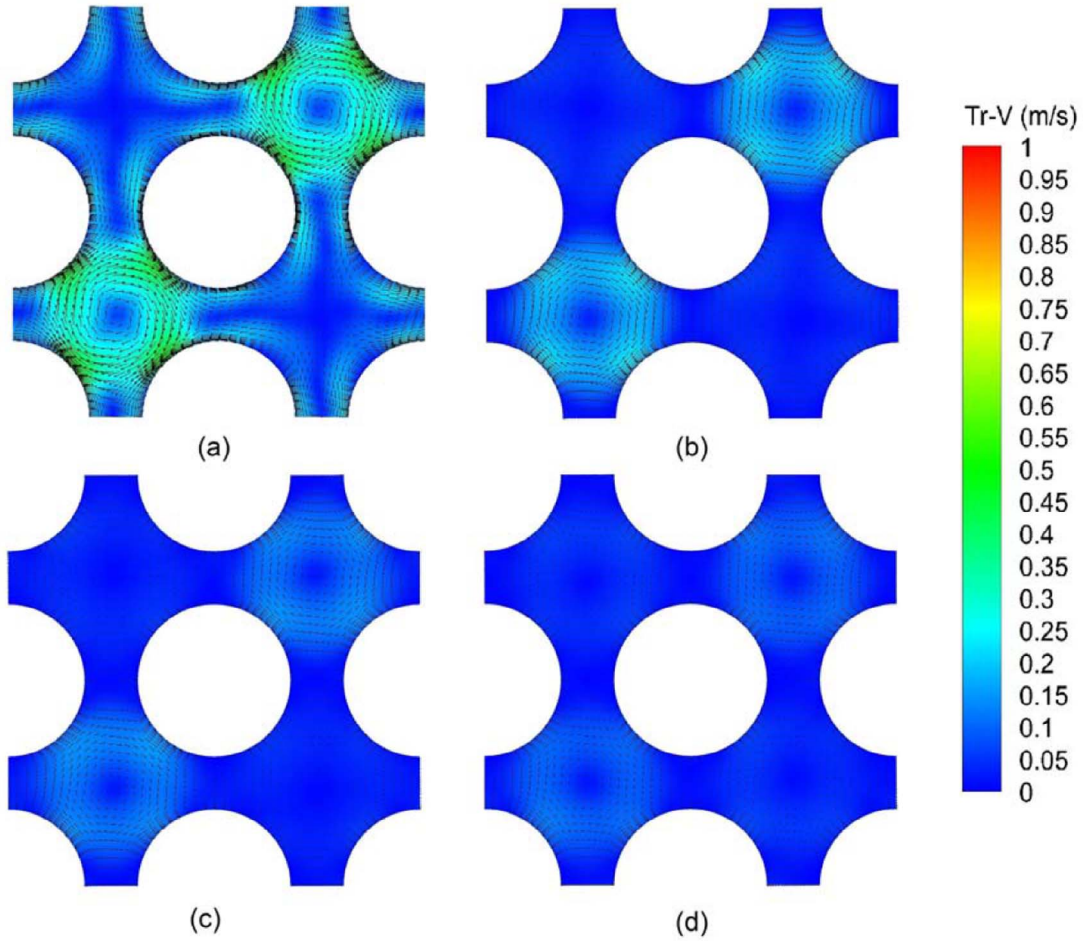

Fig. 9. Transverse velocity distribution on different cross section for the case with α = 60° (a) Y = 80 mm (b) Y = 160 mm (c) Y = 240 mm (d) Y = 320 mm.

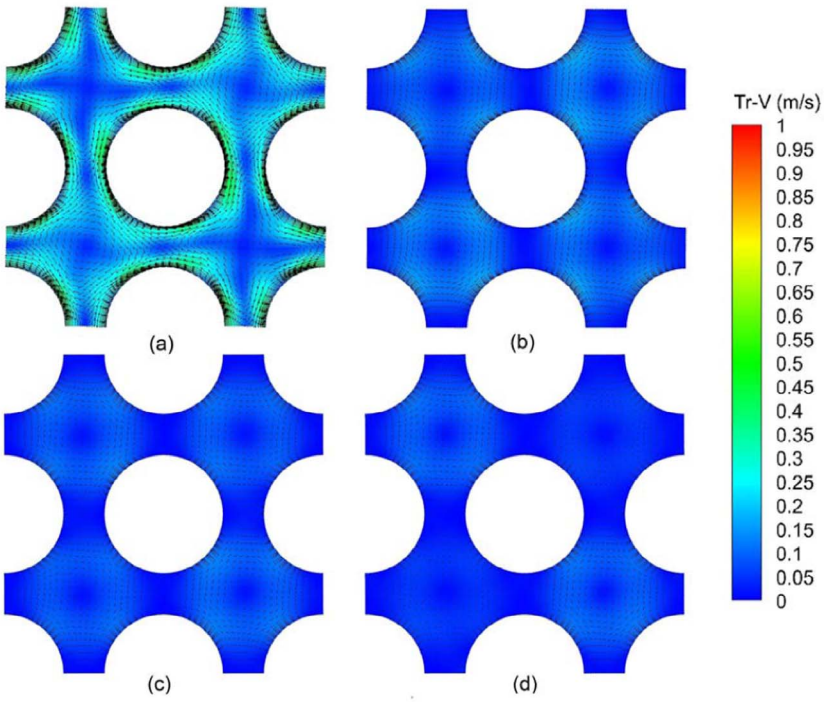

Fig. 10. Transverse velocity vector field distribution on different cross section for the case with α = 45° (a) Y = 80 mm (b) Y = 160 mm (c) Y = 240 mm (d) Y = 320 mm.

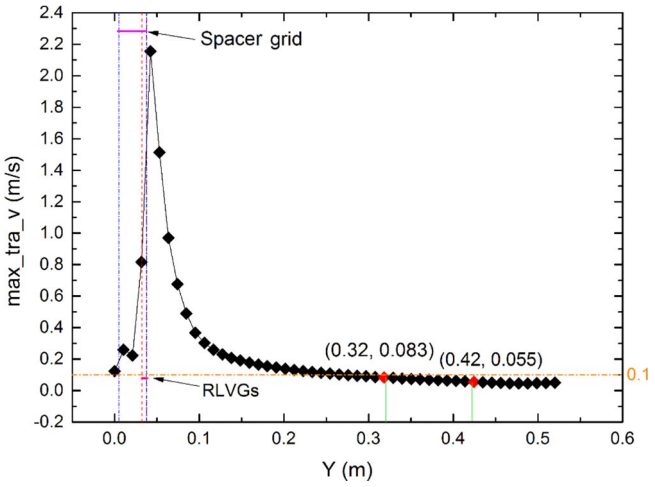

Fig. 11. Maximum transverse velocity profiles along the Y direction.

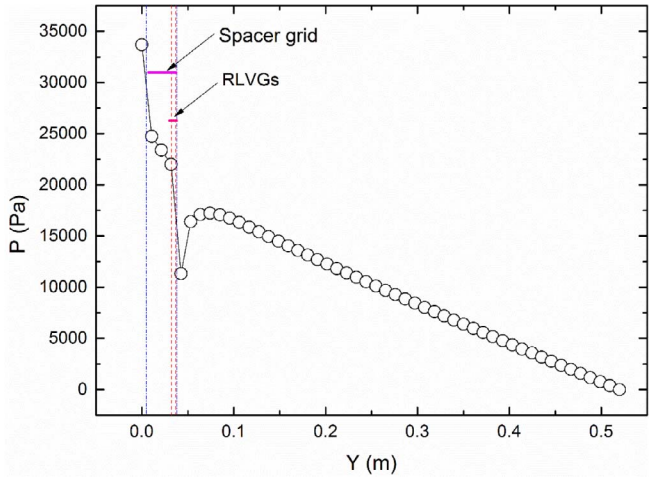

Fig. 12. Pressure profiles along the Y direction.

gradually along the Y direction. In combination with Figs. 10 and 11, it is found that the vortex phenomenon will last until the downstream of Y = 320 mm, where the maximum transverse velocity is about 0.083 m/s. When approaching Y = 420 mm, the maximum transverse velocity decreases to be about 0.055 m/s, the effect of the vortex almost disappears.

The variation of the mean pressure in sub-channels along the Y direction is shown in Fig. 12. From Y = 5 to 50 mm, where the spacer grid is located, the pressure decreases rapidly due to the local resistance of spacer grid. That is because the presence of the spacer grid reduces the flow cross-sectional area, increases the coolant velocity between the grid straps and rods, and results in extra wall frictional resistance of straps. Between 30 mm and 40 mm where the RLVGs is located, the pressure suddenly decreases due to local resistance of RLVGs. In the downstream of spacer grid, the pressure firstly picks up because the cross-sectional area becomes large, then declines gradually due to frictional drag. In this calculation the outlet is set as pressure-out boundary with a reference pressure of 1 atm, thus the gauge pressure is 0 Pa at the outlet.

Fig. 13 shows the coolant temperature distribution at different cross sections along the Y direction. It can be seen that the coolant temperature gradually increases from the inlet to the outlet due to the heat transfer from fuel rods to coolant. In the downstream of RLVGs, the temperature distribution on the cross section is not uniform due to the no-uniform distribution of vortices. The maximum temperature remains on the rods outer surface, while the minimum value of coolant temperature appears on about the center of each cross section of sub-channels.

The variation of the average wall temperature of the fuel rods for the three cases with different attack angles of RLVGs along the Y direction is given in Fig. 14. In the region upstream of the RLVGs, wall temperature rises very fast; then a decrease occurs attributing to the good cooling by the strong longitudinal vortices action. Then rod wall temperature rises gradually behind the RLVGs, the rising rate of wall temperature is less than that in section before RLVGs. This also attribute to the lasting longitudinal vortices in the sub-channels. Fig. 14 shows that the spacer grid with 45° RLVGs can brings about better cooling of the fuel rods in comparison with the cases of 30 ° and 60°.

The variation of average Nusselt numbers of the three cases with different attack angles of RLVGs along the Y direction are shown in Fig. 15. It is found that the heat transfer for the case with 45° RLVGs is better than that of 30°and 60° cases. The heat transfer of 30° case is stronger at the early stage but becomes the same at the later stage as that of the 60° case. This implies that the generated vortices by 45° RLVGs are more persistent along the Y direction and achieve better overall cooling performance.

The influence of attack angle of RLVGs on the pressure drop of sub-channels is shown in Fig. 16. The resistance coefficient is increased with the increase of attack angle of RLVGs. Combination of the heat transfer and flow loss results, it is indicated that the spacer grid with RLVGs in attack angle of 45° could behave better.

3.2. Modification on the distribution of rectangular wing longitudinal vortex generators

3.2.1. Improvement on the distribution of RLVGs on the spacer grid-pattern 2

The above numerical results show that the secondary flow induced by RLVGs in the design of pattern 1 is not so strong. In order to improve the heat transfer performance of the present spacer grid, another design of pattern 2 is proposed. The number of the punched RLVGs around each rod is increased from 2 to 4, shown in Fig. 17. The rod-grid-RLVGs units are completely identical in pattern 2 design.

3.2.2. Sensitivity analyses of the influence of turbulence models on the flow predictions

Different turbulence models are suitable to different turbulent flow simulation. For the present study, strong main longitudinal vortices with small vortices are generated in the sub-channels. Simulations used models of k-epsilon model with enhanced wall function, SST k-ω and Stress-BSL model in Reynolds stress model (RSM) for pattern 2 design are carried out and the results are compared to check the sensitivity of turbulence models on the capture of the generated vortices. The predicted vortices used the three turbulence models on two cross sections of Y = 0.065 m and Y = 0.1 m are compared in Fig. 18.

Firstly, focus on the flow characteristics on the cross section of Y = 0.065 m. It is found that strong main vortices with four smaller vortices (at the 45, 135, 225 and 315 degrees orientation) in every sub-channel are captured by the k-epsilon model shown in Fig.18(a). The main vortices in the four sub-channels are the same in clockwise, while the four smaller vortices in every sub-channel are in counterclockwise. The main vortex interacts with the four smaller vortices and improve the rotation each other. The secondary flow in the four sub-channels are almost symmetric. It is interesting to find that in the gaps between the fuel rods, coolant sweeps past the two neighboring rods surfaces with

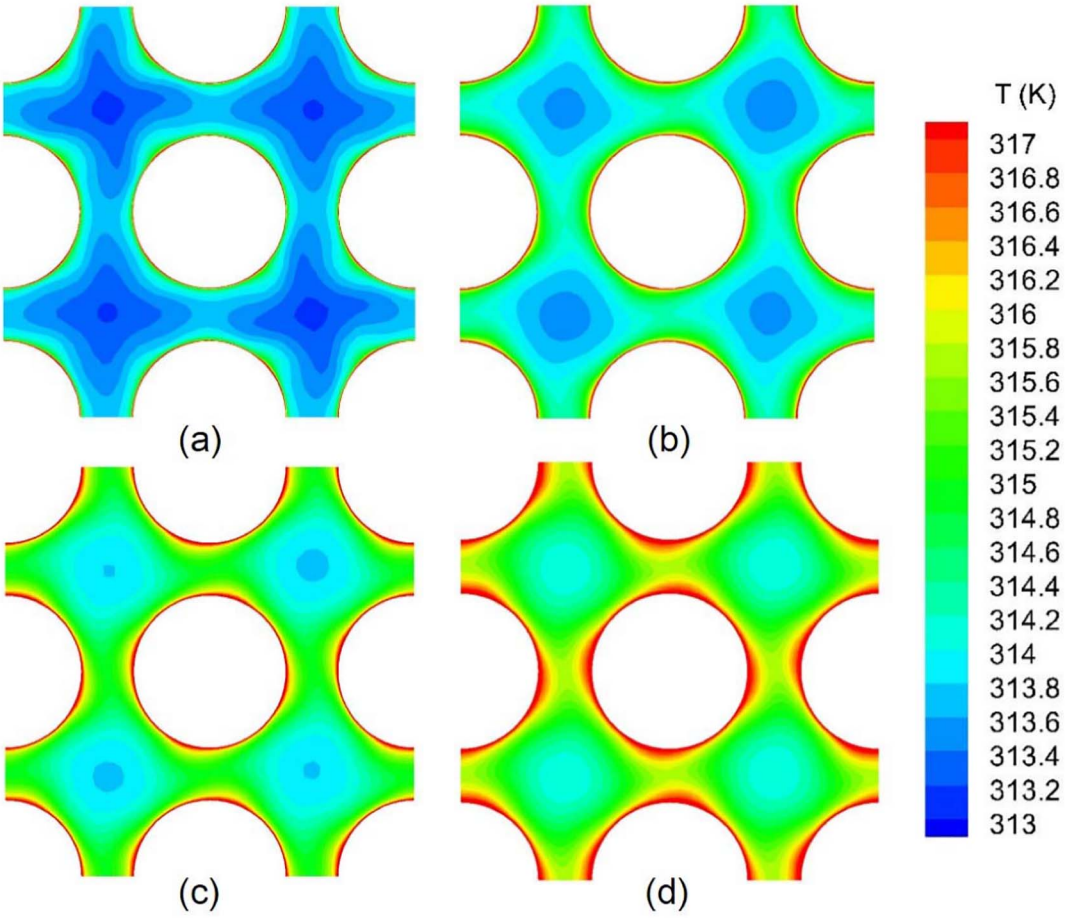

Fig. 13. Temperature contours on different cross sections (a) Y = 80 mm (b) Y = 160 mm (c) Y = 240 mm (d) Y = 320 mm.

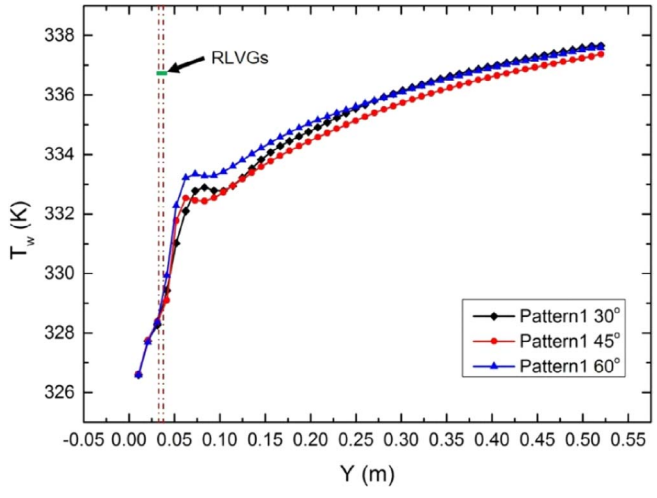

Fig. 14. Variation of average temperature of the rod wall along the Y direction.

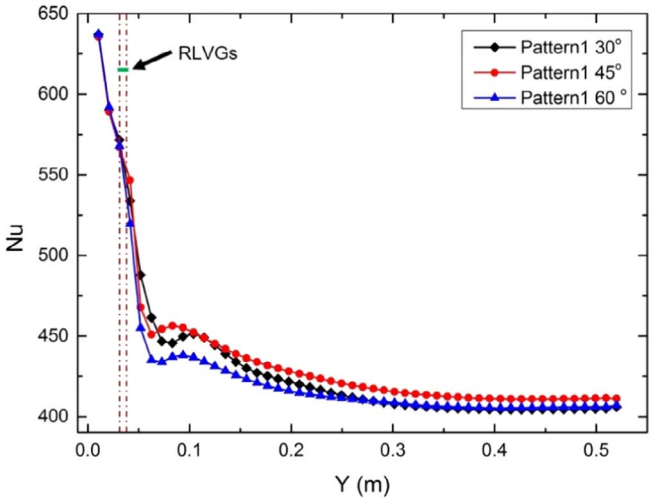

Fig. 15. Effects of RLVGs on Nu number along Y direction.

large transverse velocity but in different direction. This transverse flow could benefit to the cooling of local fuel rod. As shown in Fig.18(b) the results using SST k-ω model also reflect the same characteristics about the five vortices in every sub-channel. However, another four smaller vortices (at about 0, 90, 180 and 270 degrees orientation) are also shown in Fig.18(b). The transverse velocity in the rod gaps is larger than that in k-epsilon model's result and with obvious shear flow feature. The flow in the four sub-channel is not symmetric again. RSM model's results in Fig.18(c) also show five obvious vortices in every sub-channel as in Fig.18(a) and (b). However, the vortices at about 0, 90, 180 and 270 degrees orientation have no obvious vortex centers and with some extent deformation in comparison with SST k-ω model's results. The strong shear flow in rod gaps also could be found. The asymmetry flow in the four sub-channels is more obvious.

In comparison with the results on the cross section of Y = 0.10 m, it is found that the density of all vortices are weaken. The smaller vortices near the rod wall almost disappear. However, the sweeping flow to the

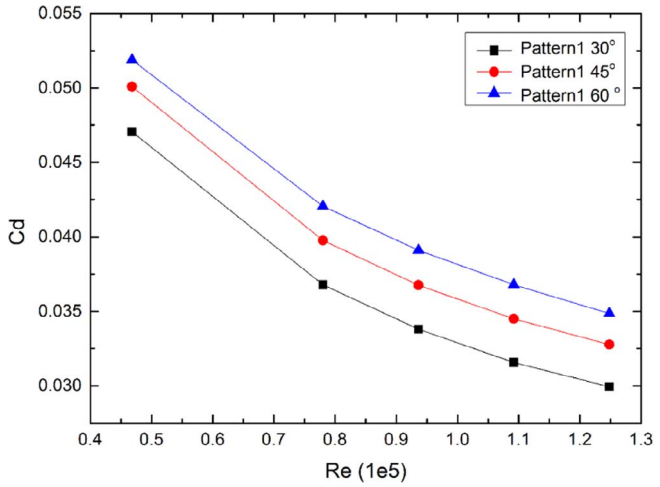

Fig. 16. Effect of attack angle of RLVGs on the pressure drop of sub-channels.

rod surfaces in the rod gaps could be found still. All these differences could be explained by the different method to handle the Reynolds stress in different turbulence models. In k-epsilon model, turbulent viscosity is taken as isotropy, some flow details are averaged. SST k-ω model could solve the flow near the walls directly, so it is good at detecting the shear flow. As about RSM model, it suits to solve the anisotropy flow even with rotation, because the Reynolds stress equation is solved directly in this model.

The effect of turbulence models on the predicted Nu along Y direction is shown in Fig. 19. It is found that k-epsilon model with enhanced wall function predicts higher Nu values along Y direction than those by SST k-ω and RSM models. While the SST k-ω and RSM models have almost the same results in the downstream of spacer grid.

Anyway, as a first step, the predicted results used k-epsilon model with enhanced wall function is adopted in the following to compare the performance between pattern 2 and pattern 1. Further simulation work used SST k-ω and RSM turbulent to optimize the spacer grid design is being carried out.

Fig. 20 compares the transverse velocity distribution of pattern 2 with that of pattern 1 at the same attack angle of RLVGs (45°) and Reynolds number (93600) on two cross sections of Y = 0.065 m and Y = 0.15 m. Just like the describing in the above text, very strong longitudinal vortices are generated which locates in the central of every sub-channel for pattern 2, shown in Fig. 20(a). Smaller vortices are also found. And in the gaps between the neighboring rods, secondary flow also is induced. In comparison with pattern 1, more zones with higher transverse velocity distributes in the rod gaps and centers of the sub-channels, the vortices spread further to the downstream of the spacer grid. Temperature distributions on two cross sections of Y = 0.065 m and Y = 0.15 m for pattern 2 and pattern 1 are compared in Fig. 21. In comparison with that of pattern 1, temperature distribution for pattern 2 is more uniform in the four sub-channels. More low temperature coolant is induced to flow across the rod gaps. This could bring about more uniform and enhanced cooling to the fuel rods.

The average transverse velocity values along Y direction between pattern 2 and pattern 1 are compared in Fig. 22. Obviously, the average transverse velocity in pattern 2 is increased much more and especially in the downstream of RLVGs in comparison with that of pattern 1. However, the average transverse velocity of Pattern 2 gradually approaches to that of pattern 1 and they are almost the same. This indicates that the action of the generated vortices is weakening along Y direction. And after Y = 0.3 m the advantage of pattern 2 is no longer exist.

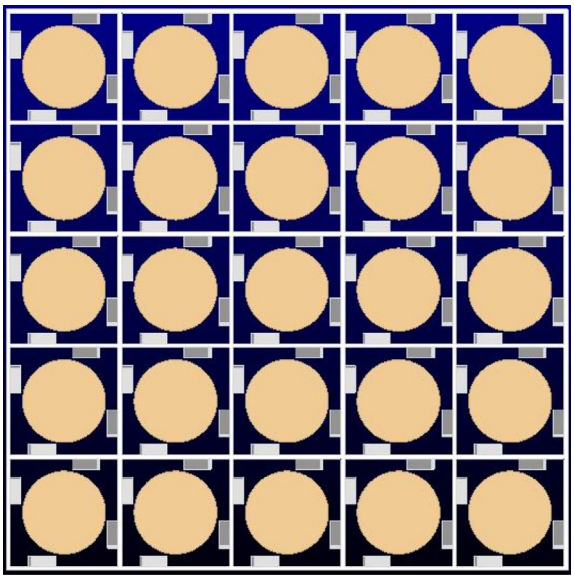

(a) Top view

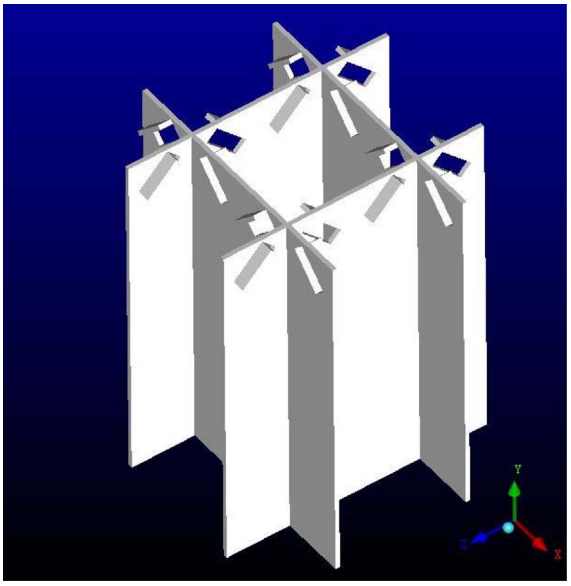

(b) Simplified axonometric drawing

Fig. 17. The schematic of the modified novel spacer grid of pattern 2.

In addition, the comparisons of the coolant bulk temperature and the average wall temperature of rods along the Y direction between patterns 2 and 1 are presented in Figs. 23 and 24. One can find from Fig. 23 that the variation of coolant bulk temperature is the same for both patterns 2 and 1 because they have same inlet mass flow rate and constant heat flux boundary on the rods surface. However, Fig. 24 shows that the average wall temperature of rods is obviously lower for pattern 2 in comparison with that of pattern 1 in the near downstream of RLVGs. After about Y = 0.3 m, they become almost the same, just like the variation of average transverse velocity. Figs. 25 and 26 compare the differences on the average Nu number and the flow resistance

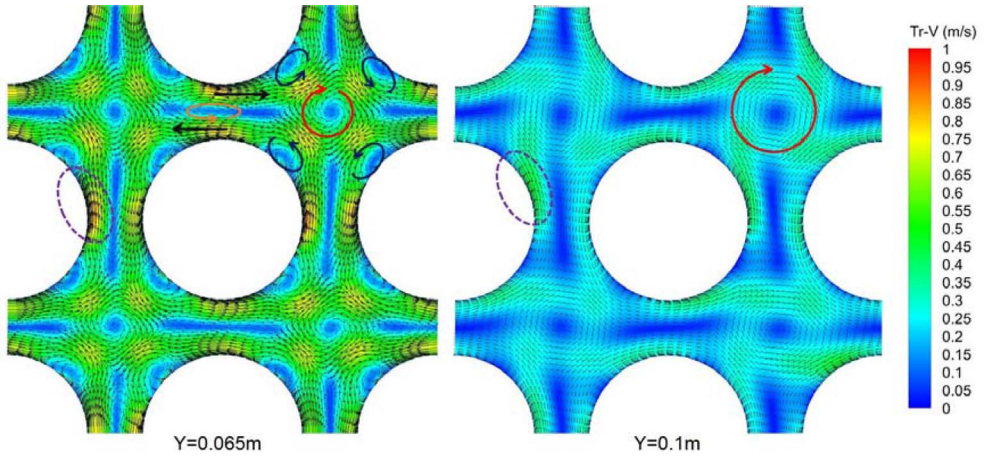

(a) k-epsilon model with enhanced wall function

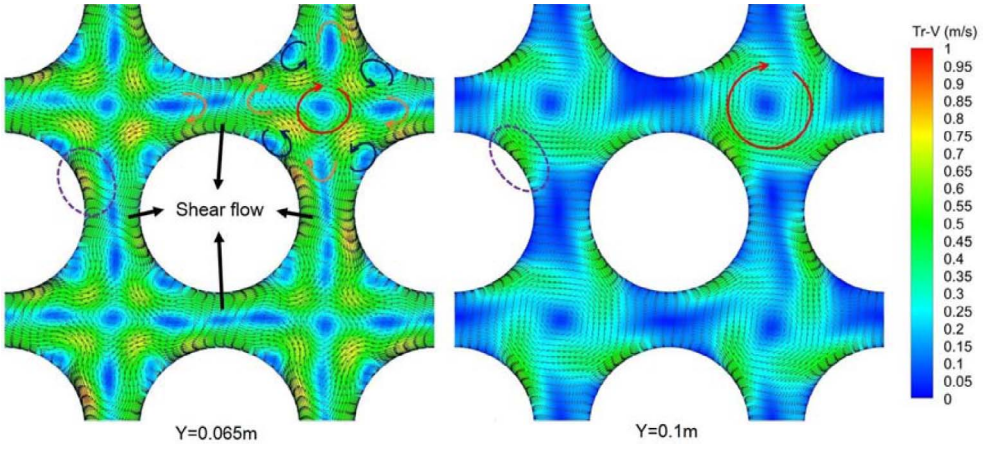

(b) SST k-ω model

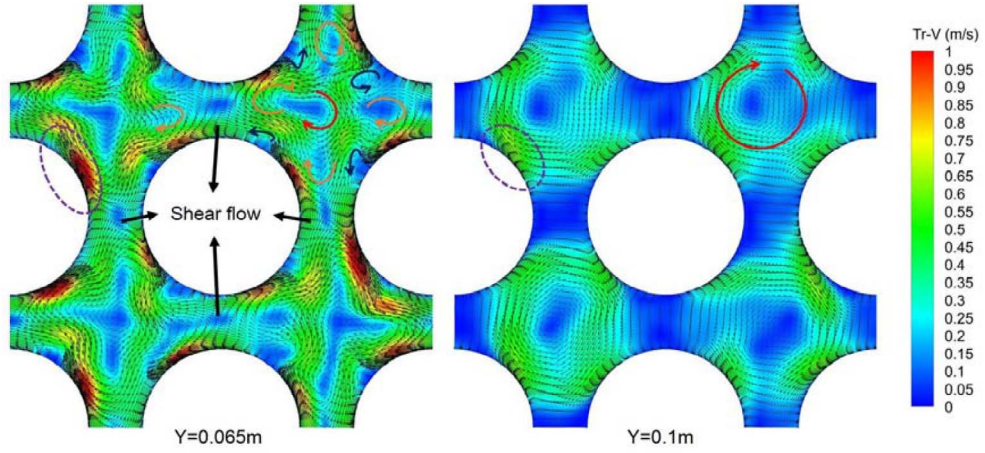

(c) RSM model

Fig. 18. Effect of turbulence model on the predicted flow characteristics.

along the Y direction between the patterns 2 and 1. Fig. 25 shows that the pattern 2 greatly improves the heat transfer in the sub-channels in the near downstream of RLVGs. Maximum increase in Nusselt number for pattern 2 in comparison with that of pattern1 is up to about 30%. This increase will last until Y exceeds 0.3 m. This accords with the variation of rod wall temperature. Based on these results, it is suggested that the distance between the two neighboring spacer grids should be decreased so as to relay the action of longitudinal vortices on the cooling enhancement when this novel spacer grid is applied in practical fuel assembly. As a penalty, the pressure drop of pattern 2 is increased in comparison with that of pattern 1 due to the increase of the number of RLVGs. The total pressure drop is increased about 7.6%. Generally,

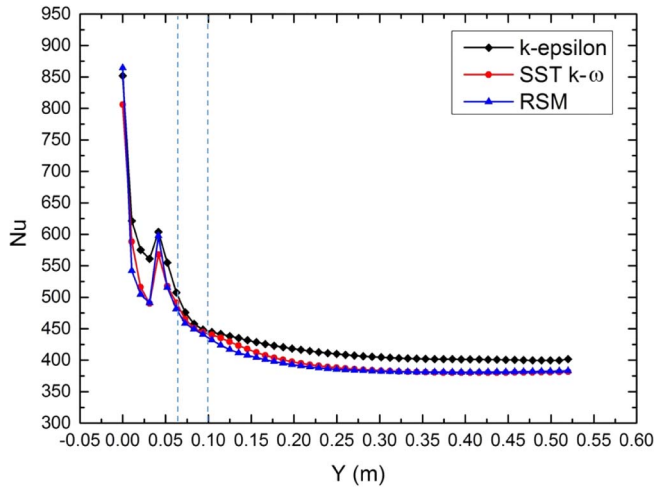

Fig. 19. Effect of turbulence model on the predicted Nu along Y direction.

the enhancement of heat transfer and decrease of the rod surface temperature for pattern are encouraging.

4. Conclusions

A novel design of spacer grid with the RLVGs is proposed to improve the thermal-hydraulic characteristics of fuel assembly and simplify the spacer grid structures. The impacts of the attack angle and the distribution of the RLVGs are investigated by numerical simulation. The following results can be obtained.

(1) Rectangular wing type longitudinal vortex generator punched out directly from the straps of spacer grid can causes the secondary flow and generates longitudinal vortices in the sub-channels which could spread to the far downstream region of sub-channels. The secondary flow disturbs the boundary layer of the rods and improves the cooling of fuel rods.
(2) For the CFD analysis of the anisotropy turbulence flow as caused by the RVLGs, SST k-ω and RSM turbulent models are more capable of detecting the multi-scale vortices.
(3) For design of pattern 1, RLVGs attack angles of 45° could generate more uniform and persistent longitudinal vortices in the sub-channels.
(4) For design of pattern 2, very strong longitudinal vortices are generated in every sub-channels and swirling in the same clockwise direction. In the gaps between the neighboring rods, the secondary flow is also induced. The average transverse velocity of the secondary flow is increased, while the average temperature on the rods surface is decreased in comparison with those of pattern 1 at the same conditions. The maximum increase in Nusselt number is up to 30% while the increase in total pressure drop is about 7.6%. However, after Y = 0.3 m the advantage of pattern 2 is no longer exist. It is suggested that the distance between the two neighboring

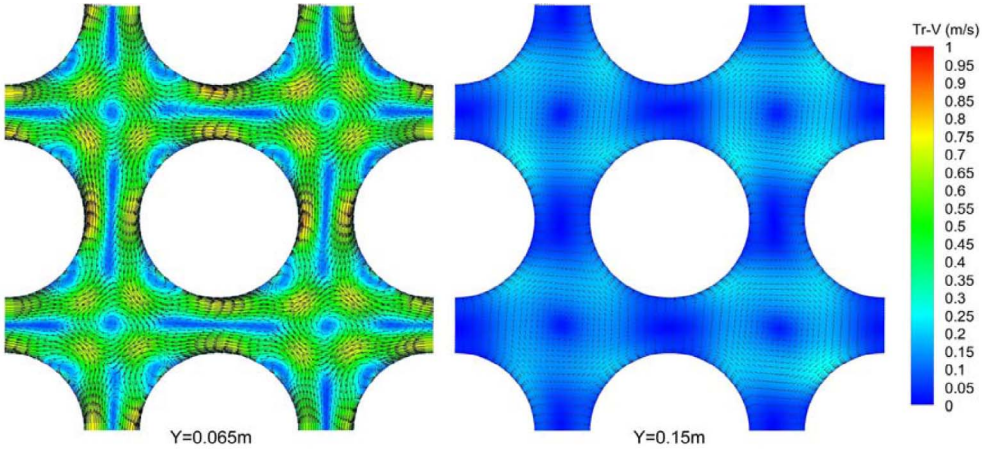

(a) Pattern 2

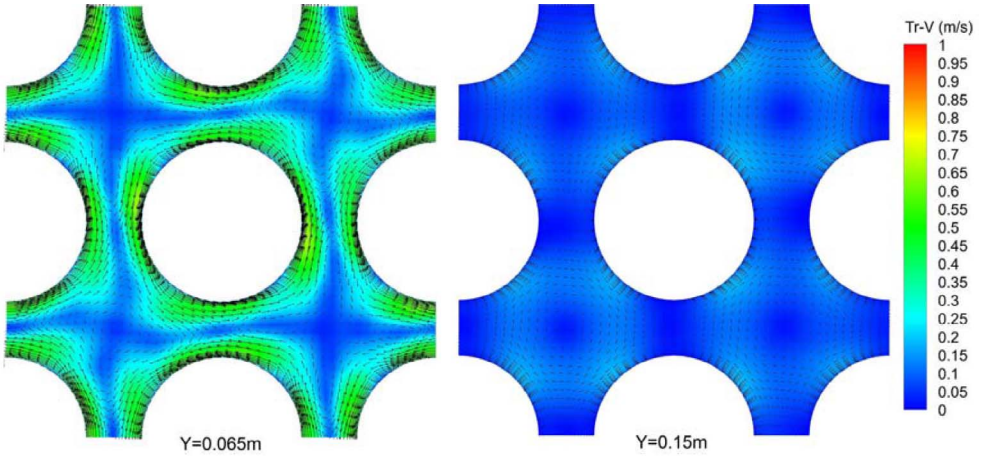

(b) Pattern 1

Fig. 20. Comparison of transverse velocity distribution between the two patterns.

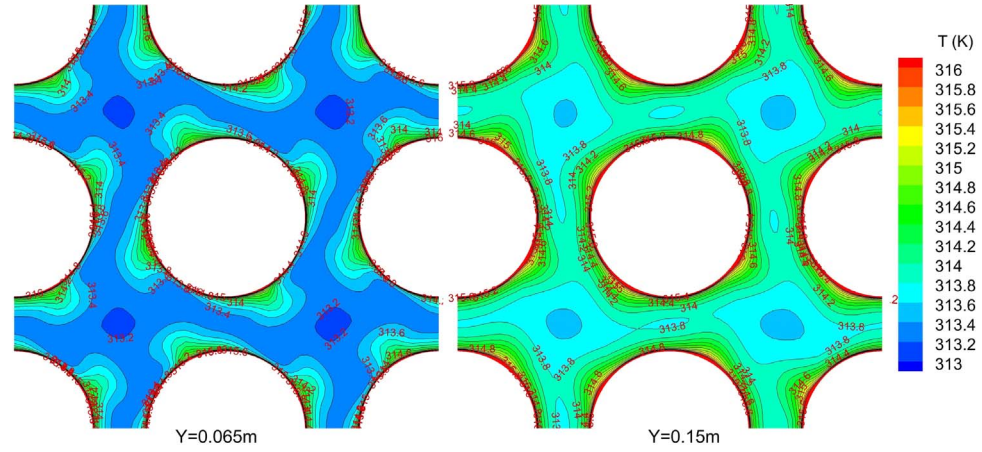

(a) Pattern 2

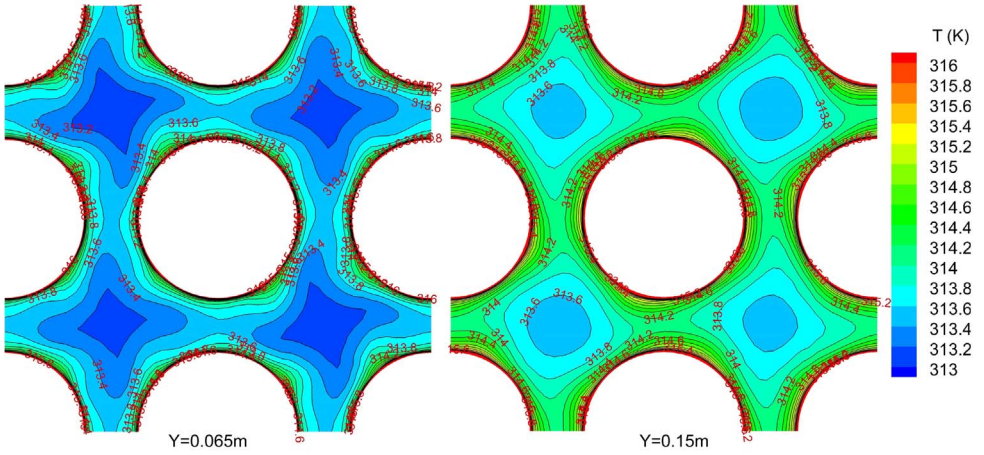

(b) Pattern 1

Fig. 21. Comparison of temperature distribution between the two patterns.

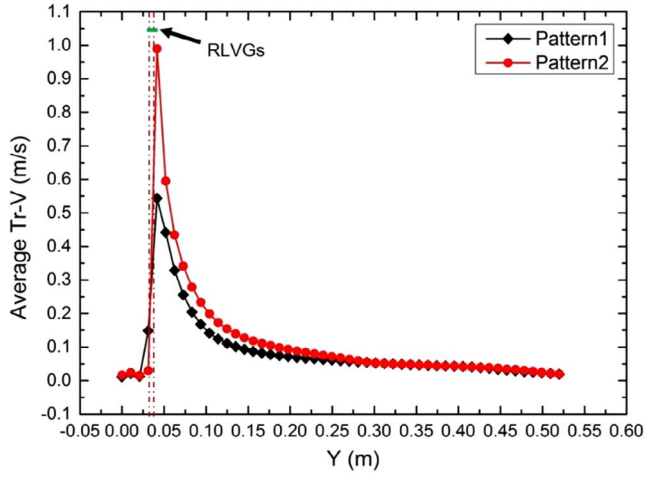

Fig. 22. Comparison of average transverse velocity values along Y direction between the two patterns.

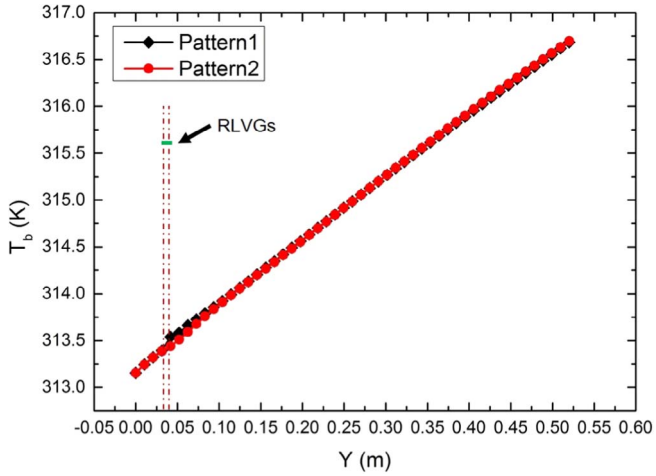

Fig. 23. Comparison of coolant bulk temperature along Y direction between the two patterns.

spacer grids should be decreased so as to relay the action of longitudinal vortices on the cooling enhancement when this novel spacer grid is applied in practical fuel assembly. The proposed design of pattern 2 deserves more attentions to optimize its structure and distribution for more heat transfer enhancement.

(5) The present simulation work tries to find some interesting secondary flow characteristic in the sub-channels induced by RLVGs on the novel spacer grid based on CFD method. The experimental work about this topic deserves to be conducted to check the reliability of the present numerical method and find the potential application of this novel spacer grid.

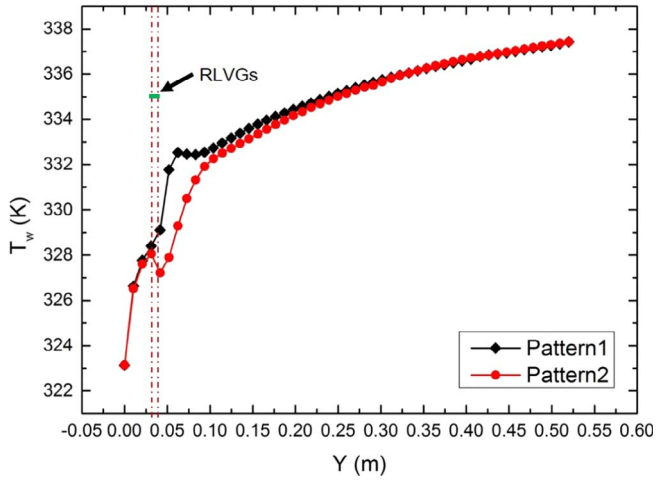

Fig. 24. Comparison of the rod wall temperature along Y direction between the two patterns.

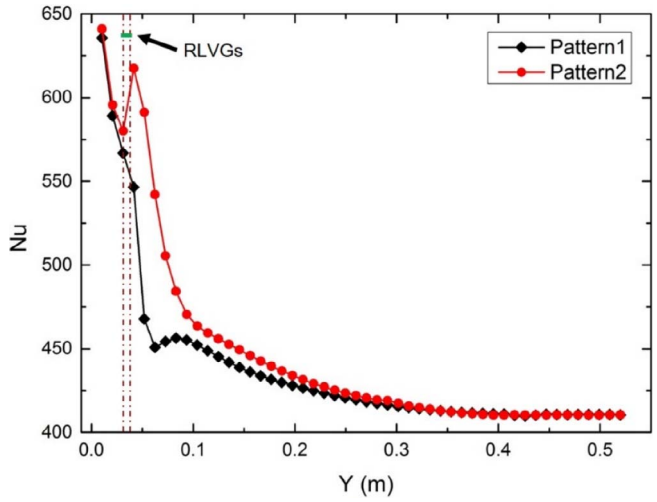

Fig. 25. Comparison of Nu number along Y direction between the two patterns.

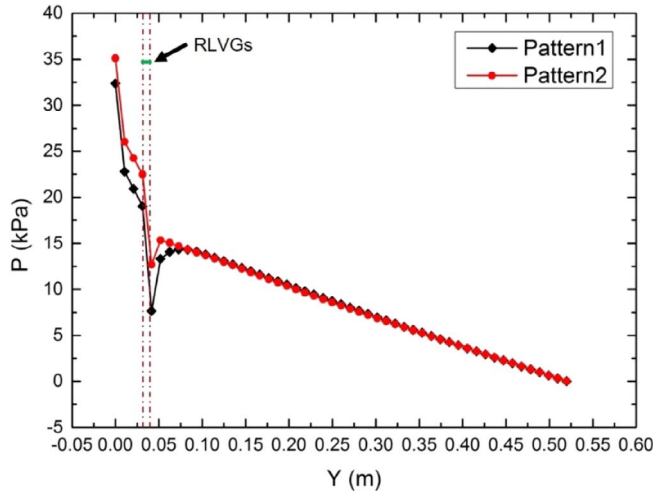

Fig. 26. Comparison of the pressure along Y direction between the two patterns.

Acknowledgements

This work is supported by the "National Natural Science Foundation of China" (Grant No. 11475133) and Program for Changjiang Scholars and Innovative Research Team in University (IRT1280).

References

Agbodemegbe, V.Y., Cheng, X., Akaho, E.H.K., Allotey, F.K.A., 2016. An investigation of the effect of split-type mixing vane on extent of cross flow between sub-channels through the fuel rod gaps. Ann. Nucl. Energy 88, 174–185.

Ahmed, H.E., Mohammed, H.A., Yusoff, M.Z., 2012. An overview on heat transfer augmentation using vortex generators and nanofluids: approaches and applications. Renew. Sustain. Energy Rev. 16, 5951–5993.

Bieder, U., Falk, F., Fauchet, G., 2014. LES analysis of the flow in a simplified PWR assembly with mixing grid. Prog. Nucl. Energy 75, 15–24.

Capone, L., Benhamadouche, S., Hassan, Y.A., 2016. Source term modeling for spacer grids with mixing vanes for CFD simulations in nuclear reactors. Comput. Fluids 126, 141–152.

Chang, D., Tavoularis, S., 2015. Hybrid simulations of the near field of a split-vane spacer grid in a rod bundle. Int. J. Heat Fluid Flow 51, 151–165.

Chang, S.K., Moon, S.K., Baek, W.P., Choi, Y.D., 2008. Phenomenological investigations on the turbulent flow structures in a rod bundle array with mixing devices. Nucl. Eng. Des. 238, 600–609.

Conner, M.E., Baglietto, E., Elmahdi, A.M., 2010. CFD methodology and validation for single-phase flow in PWR fuel assemblies. Nucl. Eng. Des. 240, 2088–2095.

Gandhir, A., Hassan, Y., 2011. RANS modeling for flow in nuclear fuel bundle in pressurized water reactors (PWR). Nucl. Eng. Des. 241, 4404–4408.

Han, S.Y., Seo, J.S., Park, M.S., Choi, Y.D., 2009. Measurements of the flow characteristics of the lateral flow in the 6×6 rod bundles with Tandem Arrangement Vanes. Nucl. Eng. Des. 239, 2728–2736.

Holloway, M.V., Beasley, D.E., Conner, M.E., 2008. Single-phase convective heat transfer in rod bundles. Nucl. Eng. Des. 238, 848–858.

Jayanti, S., Rajesh, Reddy K., 2013. Effect of spacer grids on CHF in nuclear rod bundles. Nucl. Eng. Des. 261, 66–75.

Johnson, T.R., Joubert, P.N., 1969. The influence of vortex generators on the drag and heat transfer from a circular cylinder normal to an airstream. J. Heat Transfer 91, 91–99.

Krapivtsev, V.G., Markov, P.V., Solonin, V.I., 2015. Flow and heat transfer in fuel rod bundles of water-cooled reactors with modified cell-type spacer grids. Nuclear Energy and Technology 1, 153–157.

Liu, C.C., Ferng, Y.M., Shih, C.K., 2012. CFD evaluation of turbulence models for flow simulation of the fuel rod bundle with a spacer assembly. Appl. Therm. Eng. 40, 389–396.

Nematollahi, M.R., Nazifi, M., 2008. Enhancement of heat transfer in a typical pressurized water reactor by different mixing vanes on spacer grids. Energy Convers. Manage. 49, 1981–1988.

Podila, K., Rao, Y.F., 2016. CFD modelling of turbulent flows through 5×5 fuel rod bundles with spacer-grids. Ann. Nucl. Energy 97, 86–95.

Podila, K., Rao, Y.F., Krause, M., Bailey, J., 2014. A CFD simulation of 5 × 5 rod bundles with split-type spacers. Prog. Nucl. Energy 70, 167–175.

Schubauer, G.B., Spangenberg, W.G., 1960. Forced mixing in boundary layers. J. Fluid Mech. 8, 10–32.

Shin, B.S., Chang, S.H., 2009. CHF experiment and CFD analysis in a 2×3 rod bundle with mixing vane. Nucl. Eng. Des. 239, 899–912.

Su, G.H., Qiu, S.Z., Tian, W.X., 2013. Computing Method of Thermo-Hydraulics For Nuclear Power System. Press of Tsinghua University.

Tóth, S., Aszódi, A., 2010. CFD analysis of flow field in a triangular rod bundle. Nucl. Eng. Des. 240, 352–363.

Tseng, Y.S., Ferng, Y.M., Lin, C.H., 2014. Investigating flow and heat transfer characteristics in a fuel bundle with split-vane pair grids by CFD methodology. Ann. Nucl. Energy 64, 93–99.

Wu, J.M., Tao, W.Q., 2007. Investigation on laminar convection heat transfer in fin-and-tube heat exchanger in aligned arrangement with longitudinal vortex generator from the viewpoint of field synergy principle. Appl. Therm. Eng. 27, 2609–2617.

Zhang, R., Cong, T.L., Tian, W.X., Qiu, S.Z., Su, G.H., 2015. CFD analysis on subcooled boiling phenomena in PWR coolant channel. Prog. Nucl. Energy 81, 254–263.

Zhu, X., Morooka, S., Oka, Y., 2014. Numerical investigation of grid spacer effect on heat transfer of supercritical water flows in a tight rod bundle. Int. J. Therm. Sci. 76, 245–257.